Capillary Waves in Langmuir-Blodgett Interfaces and Formation of Confined CdS Layers

J. K. Basu and M. K. Sanyal

Surface Physics Division, Saha Institute of Nuclear Physics, 1/AF Bidhannagar, Calcutta 700 064, India

(Received 9 June 1997)

Nanometer sized CdS particles can be formed by exposing cadmium arachidate Langmuir-Blodgett films to hydrogen sulphide environment. X-ray scattering studies were performed to understand the formation of these particles that exhibit the quantum confinement effect in band structure. It was observed that the CdS layers remain confined within a region of $\sim$14 Å around metal interfaces in these films. The sharp interfaces and the multilayer molecular stack of the films remains intact in the process of CdS formation. Logarithmic in-plane interfacial correlation, characteristic of capillary waves on liquid surfaces, was observed in both exposed and unexposed films. [S0031-9007(97)04769-8]

PACS numbers: 68.18.+p, 61.46.+w, 68.10.–m, 68.55.–a

Langmuir-Blodgett (LB) films are being widely studied [1–3] as model systems for exploring various physical, chemical, and biological phenomena in reduced dimension. A simple process, which involves sequential transfer of organic monolayer spread on water or other liquids by repeated dipping of a substrate, is used to form LB films. In spite of extensive research, the ease of formation of these films having exceptionally well ordered, stable molecular stack remains an enigma even 80 years after the discovery of this technique. It is well known from initial years of development of this technique that interfaces present in these films are quite rigid and sharp and one can deposit a film even on a wire mesh [4]. Although recent advances in measurement techniques, such as grazing incidence x-ray scattering [5,6] and scanning probe microscopy [1,3], and progress in the theoretical formalisms [7] to study the structure of surfaces and interfaces have improved our understanding of the structure of LB films [1,6,8–10], we still do not have a comprehensive knowledge about the exact mechanism of formation and stability of such films.

Understanding the formation of nanometer sized semiconductor particles that exhibit the finite size effect in band structure is of seminal importance [11]. It was shown recently that by exposing a cadmium arachidate (CdA) LB film in a hydrogen sulphide (H_2S) environment, cadmium sulphide (CdS) nanostructures can be formed [12,13] without much disturbance to the embedding LB structure. The band structure of these CdS nanostructures is modified considerably due to the quantum confinement effect [11–13].

Four LB films of CdA, each 9 monolayers (ML), were deposited on quartz substrates at a surface pressure and temperature of 30 mN m^{-1} and 10 °C, respectively. Of these four films, three were exposed to H_2S gas for a duration of 10, 30, and 60 mins, respectively. The details of the experimental arrangement used to prepare these LB films have been described earlier [12]. The ultraviolet–visible absorbance data on all these films were taken and the absorption edge for the H_2S exposed films was found to be at 455 ± 5 nm indicating the formation of nanocrystalline CdS in these films [11–13]. We performed specular reflectivity and diffuse scattering measurements on two of these films, namely, the as prepared (ASP) and 60 min (60M) H_2S exposed films, to understand the role of LB interfaces in the formation of CdS nanostructures.

X-ray specular reflectivity measurements were performed on these films by keeping the angle of incidence (α) equal to the angle of reflection (β) while the diffuse scattering data were taken by keeping these angles unequal [14]. The details of the experimental setup have been described earlier [15]. The incident $CuK_{\alpha 1}$ radiation was collimated by slits having horizontal and vertical apertures of 100 and 5000 μm, respectively, with the horizontal aperture determining the width of the incident beam in the scattering plane. In case of diffuse scattering measurements the scattered beam was defined in the scattering plane by a horizontal slit of aperture 100 μm placed in front of the detector. The vertical aperture of the detector slit was kept wide open to effectively integrate [14] the out of plane component, q_y, of the scattering.

For the specular reflectivity measurement we found that the intensity of the multilayer Bragg peaks in both the films increases with increasing horizontal detector slit width even beyond the beam divergence width. Moreover, in a log-log plot the scattered intensity was found to decay linearly, with a slope $(\eta - 1)$, as a function of the in-plane scattering vector q_x, where η depends on q_z. It is also evident that the longitudinal off-specular scans follow the specular profile quite closely. These results clearly indicate that we are dealing with scattering which has a strong diffuse component around the specular ridge similar to that observed in scattering from liquid surfaces having capillary waves [14,16] with logarithmic height-height correlation [14] and multiple interfaces present in the system are highly correlated [17]. It is known that beyond a certain critical in-plane length r_c, interfaces in organic multilayer films, such as liquid crystals [18,19]

and soap films [20], behave as a correlated system, exhibiting a single logarithmic height-height correlation for all the interfaces. The value of r_c depends on the compressibility of the film and decreases with decreasing compressibility [19,20]. Hence, in analogy with these theoretical formulations and using our earlier expression [14] for liquid surfaces we can write down the height difference correlation function [7], $g(r)$, for the interfaces present in our LB films as

$$g_{ij}(r) = \sigma_i^2 + \sigma_j^2 + B\gamma_E + B\ln(\kappa r/2), \quad (1)$$

where σ_i, σ_j are the rms roughnesses of the ith and jth interfaces, B is given by $k_BT/\pi\gamma$, and κ is the low wave vector cutoff for capillary waves in LB films decided by van der Waals interactions and can be written as [21,22] $\kappa^2 = A/2\pi\gamma d^4$, where A is the effective Hamaker constant, γ is the interfacial tension, and d is the total film thickness.

Using a Gaussian resolution function for q_x, obtained from direct beam profile, we can write the expression [7,14] for the detected scattered intensity, $I(q_x, q_z)$, in terms of the Kummer function and gamma function as

$$I = I_0 \frac{R_B(q_z)q_z}{2k_0 \sin\alpha} \frac{1}{\sqrt{\pi}} \Gamma\left(\frac{1-\eta}{2}\right) {}_1F_1\left(\frac{1-\eta}{2}; \tfrac{1}{2}; \frac{q_x^2L^2}{4\pi^2}\right) + D, \quad (2)$$

where D is the constant background, arising mainly due to detector dark counts here, $R_B(q_z)$ is the specular reflectivity for a multilayer in the Born approximation [7,17,23], while the other terms are as explained in [14]. In specular condition [$q_x = 0$], Kummer function becomes unity and $2k_0 \sin\alpha$ cancels with q_z; Eq. (2) gives us effective reflectivity, $R_{\text{eff}}(q_z)$ as given in [14]. In order to avoid low q divergence, inherent in the Born approximation formalism, we have replaced $R_B(q_z)$ in Eq. (2) by $R_P(q_z)$, the reflectivity profile of a rough multilayer structure calculated using a slicing technique [24–26] to analyze our data.

The effective roughness, $(\sigma_{\text{eff}})_i$, for each interface can be written as

$$(\sigma_{\text{eff}})_i^2 = \sigma_i^2 + \frac{1}{2}B\gamma_E - \frac{1}{2}B\ln(2\pi/\kappa L), \quad (3)$$

where the true roughness σ_i is given by [14,16]

$$\sigma_i^2 = (\sigma_0)_i^2 + \frac{1}{4}B\ln\left(\frac{q_u^2 + \kappa^2}{\kappa^2}\right). \quad (4)$$

Equation (4) is a general expression for interfacial roughness, where $(\sigma_0)_i$ represents uncorrelated intrinsic roughness of the ith interface, which is neglected here as we are working in the completely correlated region; q_u is the upper wave vector cutoff of capillary waves.

Specular reflectivity and transverse and longitudinal diffuse scattering data of both films were analyzed using Eq. (2) with constant background D as 0.035 counts/sec. Although there is an uncertainty in the value of the effective Hamaker constant [22] and hence, in our case, the value κ, we have used κ as 2.6×10^{-5} Å^{-1} (taking $A = 10^{-20}$ J, $\gamma = 62.8$ mN m^{-1}, and $d = 250$ Å). It is interesting to note in Eq. (3) that the actual roughness of an interface σ_i is more than the measured effective roughness $(\sigma_{\text{eff}})_i$. However, a higher value of the van der Waal's cutoff, used here, as compared to the gravitational cutoff for the liquid-vapor interface [14], makes this difference marginal.

In Figs. 1(a) and 2(a) the specular reflectivity data along with the fit (solid line) for both the films are shown. The reflectivity profile fitted using simplified models (dashed line) is also shown. In the simplified model the number of slices used to calculate the reflectivity is minimized. The simplified model in both the films indicates the increase in the absolute values of electron densities in each bilayer as a function of depth, possibly resulting from increased disorder and formation of patches due to incomplete film coverage [27], towards the top of the film [$z = 0$ in Figs. 1(c) and 2(c)]. The electron density profile (edp) obtained from simplified and detailed models is shown in Figs. 1(c) and 2(c) where the metal sites are indicated by the higher electron density boxes.

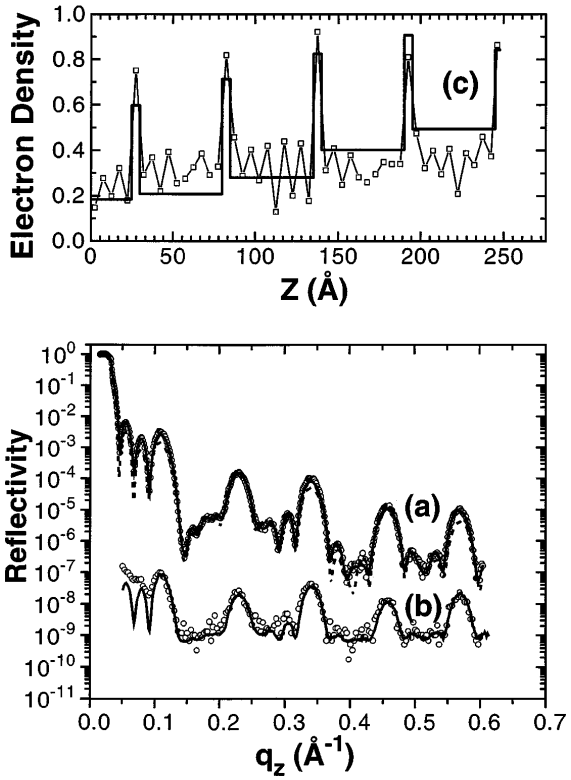

FIG. 1. (a) Specular reflectivity, (b) off-specular longitudinal, and (c) obtained electron density (electrons/Å^3) profile for as prepared film are shown. The dashed line in (a) is obtained by fitting a simple model shown in solid line in (c); the solid line in (a) is a fit of a detailed model shown in open boxes in (c). The line joining these boxes is provided only as a guide to the eye and does not provide roughness. The solid line in (b) is the calculated profile for longitudinal scattering as described in text.

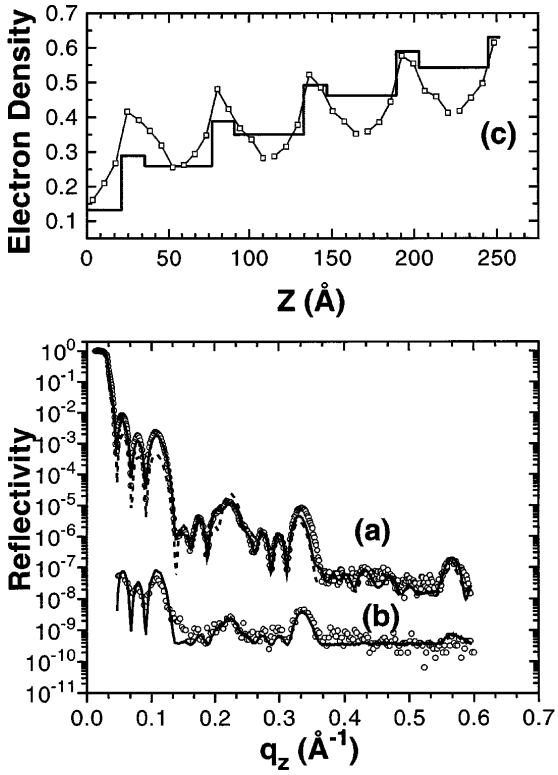

FIG. 2. (*a*) Specular reflectivity, (*b*) off-specular scattering, and (*c*) obtained electron density (electron/Å^3) profile for the 60 min exposed film are shown. Other details are as described in the caption of Fig. 1.

In the detailed model of ASP film 49 slices of 5 Å and one slice of 2.5 Å, near the substrate were used. For the 60M film we used 36 slices each having a thickness of 7 Å. It is interesting to note that the simple model for both unexposed and exposed films generates the essential features, the reflectivity profiles, while the detailed model takes care of finer details by variation of electron densities around the simple model. Using a box size of 14 Å, which is a quarter of the bilayer thickness, at the metal sites in the 60M film the simple model correctly brings out the most prominent feature in the measured reflectivity profile, i.e., vanishing of the fourth Bragg peak. The values of σ_{eff} obtained from the fitting of the simplified model for both the films are 2.1 ± 0.1 Å for the air-film interface and 2.0 ± 0.2 Å for the buried interfaces and corresponding true roughness values are 2.4 and 2.3 Å. The smearing of edp across the interfaces occurs due to interdiffusion of CdS nanoparticles confined within 14 Å, as shown in Fig. 2(*c*), and capillary wave roughness. Both these effects are included in the calculation of $R_B(q_z)$ in Eq. (2).

The total film thickness (bilayer thickness) for the 9 ML ASP and 60M film was found to be 247.5 Å (55 Å) and 252 Å (56 Å), respectively. By integrating the edp over the total film thickness, for both the ASP [Fig. 1(*c*)] and 60M [Fig. 2(*c*)] films, we notice that the difference in the electrons per unit area, for each bilayer, between the ASP and 60M films is ~1 electron/Å^2. By taking the area per molecule to be 18 Å^2 [1,6] we find that there are effectively 18 excess electrons in the 60M film as compared to the ASP film, per bilayer. This is equal to the total electrons in a H_2S molecule. In view of the above result and the fact that the molecular stacking is not disturbed, due to H_2S exposure, we conclude that the CdS nanostructures formed remain confined within the interfacial regions of the LB films around the metal sites and that there is still one metal atom within a 56 Å cylinder of cross section 18 Å^2, as indicated earlier [6].

The three sets of transverse scans (each at constant q_z) for the ASP and 60M films are shown in Fig. 3. For both the films the scans were performed at the first, second, and third Bragg peaks. For the ASP film these scans were done at q_z values of 0.108, 0.228, 0.340 Å^{-1}, respectively, while for the 60M film these scans were done at 0.107, 0.219, 0.333 Å^{-1}, respectively. The obtained value for B was 2.1 ± 0.2 Å^2 for both ASP and 60M film, giving γ as 62.8 mN m^{-1} (at 27 °C). It may be noted here that the Kummer function in

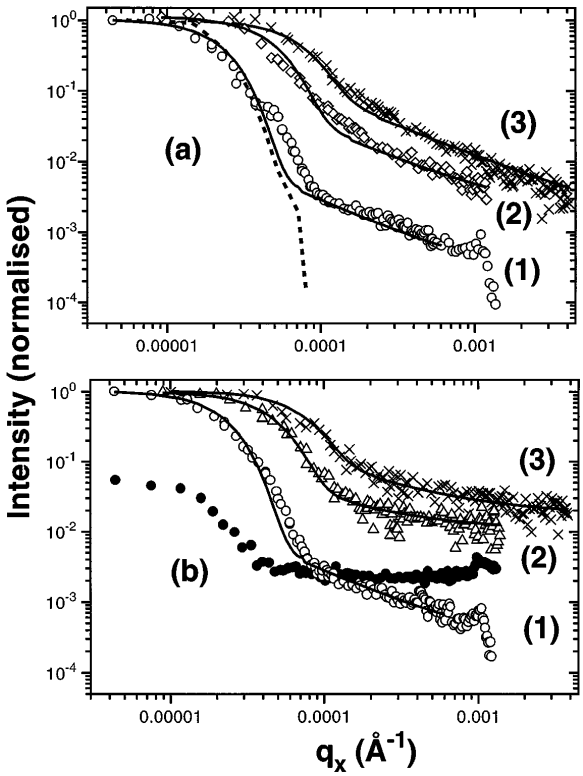

FIG. 3. Transverse diffuse scattering data for as prepared film (a) and for 60 min exposed film (b) are shown along with the fitted curves. Dashed lines in (a) indicate resolution function at first Bragg peak position. Filled circles in (b) represent the transverse diffuse scan of substrate at first Bragg peak position. All data of LB films are normalized to unity and intensity ratio of substrate and film data are shown in proper scale. Bragg peak numbers are indicated along with the respective curves (refer to text for details).

Eq. (2) not only gives the proper slope of the asymptotic diffuse scattering tail but also the proper branching point from the Gaussian shaped specular peak. This in turn decides the ratio of specular to diffuse intensity at a q_x offset. Typically, for a change in η from 0.01 to 0.1 this ratio changes by an order of magnitude (Fig. 3), and as a result gives us the sensitivity in the obtained value of B. Also plotted is the transverse scan of the bare substrate taken at $q_z = 0.107$ Å^{-1}, and the direct beam profile converted to an effective transverse resolution function at $q_z = 0.108$ Å^{-1}. It may be noted (Fig. 3) that the specular reflectivity of the substrate at $q_z = 0.107$ Å^{-1} is nearly 20 times smaller than that of the film, while the diffuse intensity is higher than that from the film. This is due to the high value of roughness of the bare substrates which was found to be 8.0 Å. Clearly the effective roughness of the bare substrates gets modified during the deposition due to the attachment of the initial monolayers, otherwise we would not have observed clear total film oscillations in the reflectivity data (refer to Figs. 1 and 2).

In Figs. 1 and 2 along with the specular data, we have shown the longitudinal diffuse data taken with a constant angular offset of 1.0 and 0.7 mrad for the ASP film [Fig. 1(b)] and for the 60M film [Fig. 2(b)], respectively. The parameters obtained from the fitting of transverse diffuse and specular data were used to calculate longitudinal diffuse scattering profiles shown in the respective figures to check self-consistency of the analysis scheme. The excellent agreement of the calculated profile with the measured data demonstrates the assumed conformality of the interfaces above the critical length scale r_c. The estimated value of r_c ($= 2\pi/q_u$) from Eq. (3) comes out to be about 1000 Å. This value in turn gives us an estimate of the compressibility, given by $2\gamma d/r_c^2$ [19], of the film as 3×10^5 N m^{-2}. Thus, the highly incompressible and sharp interfaces in LB films confine CdS molecules, formed by chemical reaction [12,13], within a region of thickness ~14 Å, at each interface, without disturbing the multilayer molecular stack in the film.

Size of semiconductor nanoparticles is generally estimated from band structure using isolated cluster models. It will be very illustrative to calculate band structure of such conformal interfaces having 14 Å layers of CdS, as we found that CdS nanoparticles of about 60 Å diameter, estimated from isolated cluster calculation, cannot exist in 56 Å thick ordered bilayers of LB films [13]. A detailed study to understand the reason for the presence of different in-plane correlation [8–10] in LB interfaces is underway. Our preliminary results show that films deposited in identical conditions on silicon indicate self-affine in-plane correlation, as found earlier [10], in contrast to films deposited on quartz substrate, presented here, exhibiting logarithmic correlation characteristic of capillary waves, as if picked up during deposition, along with the Langmuir monolayer spread on water surface.

It is our pleasure to acknowledge the help of Professor S. S. Major, and N. Prashanth Kumar and Dr. Alokmay Datta for their help in preparation of the samples and for valuable discussions. We also thank Professor Bikash Sinha for his continuous support in this activity.

[1] J. Zasadzinski *et al.,* Science **263**, 1726 (1994).
[2] *Langmuir -Blodgett Films,* edited by G. Roberts (Plenum, New York, 1990).
[3] J. A. DeRose and R. M. Leblanc, Surf. Sci. Rep. **22**, 73 (1995).
[4] G. L. Gaines, Jr., *Insoluble Monolayers at Gas-Liquid Interface* (Wiley, New York, 1966).
[5] J. Als-Nielsen *et al.,* Phys. Rep. **246**,251 (1994); J. Als-Nielsen and G. Materlik, Phys. Today **48**, No. 11, 34 (1995).
[6] A. Malik *et al.,* Phys. Rev. B **52**, R11 654 (1995).
[7] S. K. Sinha *et al.,* Phys. Rev. B **38**, 2297 (1988); S. Dietrich and A. Haase, Phys. Rep. **260**, 1 (1995).
[8] R. E. Geer *et al.,* Phys. Rev. Lett. **71**, 1391 (1993); R. E. Geer and R. Shashidhar, Phys. Rev. E **51**, R8 (1995).
[9] V. Nitz *et al.,* Phys. Rev. B **54**, 5038 (1996).
[10] A. Gibaud *et al.,* Phys. Rev. Lett. **74**, 3205 (1995).
[11] L. Brus, J. Phys. Chem. **90**, 2555 (1986); M. V. Rama Krishna and R. A. Friesner, J. Chem. Phys. **95**, 8309 (1991).
[12] A. Dhanabalan *et al.,* Solid State Commun. **99**, 859 (1996).
[13] E. S. Smotkin *et al.,* Chem. Phys. Lett. **152**, 265 (1988); N. J. Geddes *et al.,* J. Phys. Chem. **97**, 13 767 (1993); P. Facci *et al.,* Proc. Natl. Acad. Sci. U.S.A. **93**, 10 556 (1996).
[14] M. K. Sanyal *et al.,* Phys. Rev. Lett. **66**, 628 (1991).
[15] M. K. Sanyal *et al.,* Europhys. Lett. **36**, 265 (1996); S. Banerjee *et al.,* Phys. Rev. B **54**, 16 377 (1996).
[16] A. Braslau *et al.,* Phys. Rev. A **38**, 2457 (1988); D. Schwartz *et al.,* Phys. Rev. A **41**, 5687 (1990); B. M. Ocko *et al.,* Phys. Rev. Lett. **72**, 242 (1994).
[17] S. K. Sinha *et al.,* Physica (Amsterdam) **198B**, 72 (1994).
[18] R. Holyst, Phys. Rev. A **44**, 3692 (1991).
[19] E. A. L. Mol *et al.,* Phys. Rev. E **54**, 536 (1996).
[20] J. Daillant and O. Belorgey, J. Chem. Phys. **97**, 5824 (1992); **97**, 5837 (1992).
[21] I. M. Tidswell *et al.,* Phys. Rev. Lett. **66**, 2108 (1991).
[22] M. Sferraza *et al.,* Phys. Rev. Lett. **78**, 3693 (1997).
[23] M. K. Sanyal *et al.,* Mater. Res. Soc. Symp. Proc.**237**, 393 (1992).
[24] L. G. Parratt, Phys. Rev. **95**, 359 (1954).
[25] M. K. Sanyal *et al.,* J. Synchrotron Radiat. **4**, 185 (1997).
[26] M. Piecuch and L. Nevot, Mater. Sci. Forum **59/60**, 93 (1990).
[27] M. K. Sanyal *et al.,* Europhys. Lett. **21**, 691 (1993).